

Implementation and assessment of advanced failure criteria for composite layered structures in FEMAP

Amedeo Grasso¹, Pietro Nali² and Maria Cinefra*¹

¹Mechanical and Aerospace Engineering Department, Politecnico di Torino, Italy

²Thales Alenia Space, Strada Antica di Collegno, 253, 10146, Turin, Italy

(Received May 19, 2018, Revised August 31, 2018, Accepted September 6, 2018)

Abstract. AMOSC (Automatic Margin Of Safety Calculation) is a SW tool which has been developed to calculate the failure index of layered composite structures by referring to the cutting edge state-of-the-art LaRC05 criterion. The stress field is calculated by a finite element code. AMOSC allows the user to calculate the failure index also by referring to the classical Hoffman criterion (which is commonly applied in the aerospace industry). When developing the code, particular care was devoted to the computational efficiency of the code and to the automatic reporting capability. The tool implemented is an API which has been embedded into Femap Siemens SW custom tools. Then, a user friendly graphical interface has been associated to the API. A number of study-cases have been solved to validate the code and they are illustrated through this work. Moreover, for the same structure, the differences in results produced by passing from Hoffman to LaRC05 criterion have been identified and discussed. A number of additional comparisons have thus been produced between the results obtained by applying the above two criteria. Possible future developments could explore the sensitivity of the failure indexes to a more accurate stress field inputs (e.g. by employing finite elements formulated on the basis of higher order/hierarchical kinematic theories).

Keywords: API; visual basic programming; FEMAP; material science; classical/advanced failure criteria

1. Introduction

In the aerospace and aeronautic industry, the use of composite material is growing each year, and, the methodology for designing high-performance structures of composite materials is still evolving. As a matter of fact, further advances in the use of laminated composites are subordinate to a better understanding of their failure mechanisms. In this context, having a physical model for each failure mode becomes an important point of concern, because these physical models should establish when the failure takes place and describe also the post-failure behavior.

However, the analysis and simulation of the failure in composite laminated structures are quite cumbersome tasks. As anticipated by Puck (Deuschle and Puck 2013), who paid particularly attention to the differences in tensile and compressive strength, the failure mechanisms are very different from those of traditional metallic structures. The combination of various interfaces (fiber, matrix, layers) on a macro scale level requires a local dedicated analysis to establish the initiation

*Corresponding author, Professor, E-mail: maria.cinefra@polito.it

of failure mechanisms in a fiber, a crack in the matrix or a delamination between two different layers.

Moreover, in composite structures, which can accumulate damage before structural collapse, the use of failure criteria is not sufficient to predict ultimate failure. Simplified models, such as the ply discount method, can be used to predict ultimate failure, but they cannot represent with satisfactory accuracy the quasi-brittle failure of laminates that results from the accumulation of several failure mechanisms.

The study of the non-linear response of quasi-brittle materials due to the accumulation of damage is important because the rate and direction of damage propagation defines the damage tolerance of a structure and its eventual collapse. Several theories have been proposed for predicting both the initial and the progressive failure of composites (Nali and Carrera 2011). Although significant progress has been made in this area, there is currently no single theory that accurately predicts failure at all levels of analysis, for all loading conditions and all types of fiber reinforced polymer (FRP) laminates. In fact, the mechanisms that lead to failure in composite materials have not been fully understood yet. This is especially true for compression failure, for both the matrix and fiber dominated failure modes. For instance, a physical model for matrix compression failure should predict that failure occurs when a certain stress state is achieved, as well as which kind of orientation should have the fracture plane and how much energy the crack formation should dissipate.

In general, the greatest difficulty in the development of an accurate and computationally efficient numerical procedure to predict damage growth concerns with the way in which the material micro-structural changes should be analyzed and how those changes should be related to the material response. While some failure theories have a physical basis, most theories represent attempts to provide mathematical expressions that give a best fit of the available experimental data in a form that is practical from the design point of view.

The World Wide Failure Exercises (WWFEs) provided an exhaustive assessment of the theoretical methods for predicting material initial failure in Fiber Reinforced Polymer composites (FRP). It underlined that, even when analyzing simple laminates that have been extensively studied and tested, the predictions of most theories diverge significantly from the experimental observations. During the first edition of WWFE (1996) the Puck failure criterion was indicated as one of the most effective, being the predicted failure envelopes in good correlation with the test results. After WWFE II (Kaddour *et al.* 2013), NASA Langley Research Center revisited existing failure theories in order to identify the most accurate models and, if possible, to introduce some enhancements. The result of these activities is a series of criteria named LaRC. Nowadays, the LaRC05 criterion is defined by extending the approach to three-dimensional stress states (Kaddour and Hinton 2013). In the second chapter of this work, the reader can find a review of Hoffman criterion and LaRC05 criteria.

Beside the growth of knowledge, the development of new and less approximate failure theories allow the industries to design structural components with minor safety margins, thus reducing production costs. This is due to:

- less amount of material to be used;
- lower weights needed in flight;
- more detailed expectation of failure and its prevention.

However, in modern CAE software, classical failure theories have been implemented. Furthermore, the companies are skeptical about improving and using new theories. For these reasons an API for FEMAP software was implemented in the framework of this work, in which

both classical (Hoffman) and more recent (LaRC05) failure theories have been implemented to evaluate failure index.

2. Failure criteria

Different failure criteria have been formulated in order to predict failure loads for general stress states. In this text, a classification of failure criteria is proposed, in which they can be grouped in two main groups:

- Failure criteria neglecting interactions between different stress components.
- Failure criteria considering interactions between different stress components.

In the next paragraphs, an overview of these criteria is given and the analytic definition of Hoffman criterion and LaRC05 criteria is provided.

Criteria belonging to the first group are the simplest ones and they usually propose one inequality for each of the three in-plane stresses (or strain) components.

In the remaining criteria, the failure in one direction may be sensitive to loads along other directions (including shear).

This last group can be divided into the following two subgroups:

- Criteria proposing one single inequality to define the failure envelope.
- Criteria proposing a combination of interactive and non-interactive conditions.

The Hoffman, Tsai-Wu, Liu-Tsai and Tsai-Hill are quadratic criteria and they belong to the first group, while the Hashin and Rotem, Hashin, Puck and Schuermann and LaRC criteria pertain to the second one.

In general, one Failure Index (FI) corresponds to each failure criteria. A FI exceeding the unitary value means that failure occurs, according to the applied criterion.

Some useful definitions are reported for a better understanding of the following concepts:

- *Failure indices* represent a phenomenological failure criterion in which only an occurrence of failure is indicated, not the mode of failure.
- *Strength ratio* is a more direct indicator of failure than the failure index, since it demonstrates the percentage of applied load to the failure criteria. Strength ratio is defined as: Strength Ratio (SR) = Allowable Stress / Calculated Stress.

For example, a SR = 0.75 not only indicates that a failure has occurred, but also indicates that the applied load is 25% beyond the allowable. A FI = 1.25 on the other hand does not represent a percentage of failure; just that a failure condition exists.

2.1 Hoffman criterion

The following formulas were extracted by Hoffman (1967) and NX Nastran User's Guide and they were implemented in the API.

The resulting failure index in Hoffman's theory for an orthotropic lamina in a general state of plane stress (2D) with unequal tensile and compressive strengths is given by

$$FI = \left(\frac{1}{X_t} - \frac{1}{X_c} \right) \sigma_1 + \left(\frac{1}{Y_t} - \frac{1}{Y_c} \right) \sigma_2 + \frac{\sigma_1^2}{X_t X_c} + \frac{\sigma_2^2}{Y_t Y_c} + \frac{\sigma_{12}^2}{S^2} - \frac{\sigma_1 \sigma_2}{X_t X_c} \quad (1)$$

Note that this theory takes into account the difference in tensile and compressive allowable stresses by using linear terms in the equation.

Table 1 Hoffman's failure index (2D) coefficients

| | |
|---------------------------------------|------------------------------|
| $F_1 = \frac{1}{X_t} - \frac{1}{X_c}$ | $F_{22} = \frac{1}{Y_t Y_c}$ |
| $F_2 = \frac{1}{Y_t} - \frac{1}{Y_c}$ | $F_{66} = \frac{1}{S^2}$ |
| $F_{11} = \frac{1}{X_t X_c}$ | |

Table 2 Hoffman's failure index (3D) coefficients

| | |
|--|--|
| $C_1 = \frac{1}{2} \left(\frac{1}{Z_t Z_c} + \frac{1}{Y_t Y_c} - \frac{1}{X_t X_c} \right)$ | $C_6 = \left(\frac{1}{Z_t} - \frac{1}{Z_c} \right)$ |
| $C_2 = \frac{1}{2} \left(\frac{1}{X_t X_c} + \frac{1}{Z_t Z_c} - \frac{1}{Y_t Y_c} \right)$ | $C_7 = \frac{1}{S_{23}^2}$ |
| $C_3 = \frac{1}{2} \left(\frac{1}{X_t X_c} + \frac{1}{Y_t Y_c} - \frac{1}{Z_t Z_c} \right)$ | $C_8 = \frac{1}{S_{13}^2}$ |
| $C_4 = \left(\frac{1}{X_t} - \frac{1}{X_c} \right)$ | $C_9 = \frac{1}{S_{12}^2}$ |
| $C_5 = \left(\frac{1}{Y_t} - \frac{1}{Y_c} \right)$ | |

To calculate the strength ratio and then the margin of safety, the following terms are defined in Table 1.

Substituting above terms into Hoffman FI equation and setting FI = 1, the following expression for SR has been obtained:

$$SR = \frac{-b + \sqrt{b^2 - 4ac}}{2a} \quad (2)$$

where:

$$\begin{aligned} a &= F_{11}\sigma_1^2 + F_{22}\sigma_2^2 + F_{66}\sigma_{12}^2 - F_{11}\sigma_1\sigma_2 \\ b &= F_1\sigma_1 + F_2\sigma_2, \quad c = -1 \end{aligned} \quad (3)$$

If complete 3D stress field of composite material is available, the following relation of failure index is used:

$$\begin{aligned} FI_{3D} &= C_1(\sigma_2 - \sigma_3)^2 + C_2(\sigma_3 - \sigma_1)^2 + C_3(\sigma_1 - \sigma_2)^2 \\ &+ C_4\sigma_1 + C_5\sigma_2 + C_6\sigma_3 + C_7\tau_{23}^2 + C_8\tau_{13}^2 + C_9\tau_{12}^2 \end{aligned} \quad (4)$$

and the new coefficients are resumed in Table 2.

In each case, the following material data are required:

- X_t, X_c are the maximum allowable stresses in the 1-direction in tension and compression;
- Y_t, Y_c are the maximum allowable stresses in the 2-direction in tension and compression;
- Z_t, Z_c are the maximum allowable stresses in the 3-direction in tension and compression;
- S_{12} is the maximum allowable in-plane shear stress;

- S_{23} is the maximum allowable 23 shear stress;
- S_{13} is the maximum allowable 13 shear stress.

2.2 LaRC05 criteria

Further development of LaRC criteria is LaRC05, which was developed during World-Wide Failure Exercise (WWFE-II). The philosophy behind the approach is that failure models and resulting criteria ought to include as much as possible the physics associated with the failure process at the micromechanical level, while still allowing for solutions to be computed for laminae and laminates. In this paragraph only the most important concept and formulas of LaRC05 will be reported and briefly described.

Similarly, to LaRC04 (see Pinho *et al.* 2005), the maximum stress failure criterion is used to predict fibre tensile failure, indeed, it has been shown to correlate well with existing experimental data:

$$FI_{FT} = \frac{\langle \sigma_1 \rangle_+}{X_T} \quad (5)$$

2.2.1 Matrix failure

The strengths associated with matrix dominated failure in a composite should not be expected to be ‘material’ properties. They are ‘structural’ properties, dependent on the thickness of the ply and on the neighboring plies in the laminate. Indeed, under the same stress state (averaged over ply thickness), the conditions for the propagation of micro-cracks are much more favorable for the case of a unidirectional (UD) laminate than for a thin ply in a multi-axial laminate neighbored by 0° plies. The thickness of the ply and the presence of neighboring plies change the boundary conditions of the fracture mechanics problem for crack growth. Matrix-dominated failure in composites has similarities to that of pure polymer. This would indicate that criteria analogous to Raghava’s (Raghava *et al.* 1973) would be amongst the most suitable to predict matrix failure in a composite. However, to predict the consequences of failure in composites, becomes extremely important knowing the fracture angle. Then, an adaptation of Mohr-Coulomb’s failure criterion for UD composite plies is used (Pinho *et al.* 2012). So, the matrix failure index is defined as:

$$FI_M = \left(\frac{\tau_T}{S_T^{is} - \eta_T \sigma_N} \right)^2 + \left(\frac{\tau_L}{S_L^{is} - \eta_L \sigma_N} \right)^2 + \left(\frac{\langle \sigma_N \rangle_+}{Y_T^{is}} \right)^2 \quad (6)$$

with failure being predicted when $FI_M = 1$.

The terms in Eq. (6) are:

- σ_N, τ_L and τ_T are the traction components in the (potential) fracture plane, and they are obtained by stress transformation.
- The strengths Y_T^{is}, S_L^{is} and S_T^{is} are the in-situ transverse tensile strength, longitudinal shear strength and transverse shear strengths, respectively. These strengths are in-situ because they depend on the thickness of the ply and on the location of the ply in the laminate (inner or outer ply). Pinho *et al.* (2012) presented the different expressions of these strengths for each possible type of micro-cracks.
- η_T and η_L in equation are the slope or friction coefficients. They are used to account for the effect of pressure on the failure response. They increase the respective shear strengths in the

presence of a compressive normal traction and reduce the respective shear strengths in the presence of a tensile normal traction. The slope or friction coefficient η_T is obtained from the pure transverse compression test as a function of α_0 . This is a material property, in fact it is the particular value of α for pure transverse compression, that can be measured experimentally. Several sources have observed that the fracture angle for either glass or carbon composites is typically in the range 51° - 55° .

$$\eta_T = -\frac{1}{\tan(2\alpha_0)} \quad (7)$$

while the slope or friction coefficient η_L is an independent material property that needs to be measured experimentally, however an analytic relation with η_T is proposed in previous LaRC criteria.

- The term $\langle\sigma_N\rangle_+$ in the criterion represents the contribution from the positive normal traction in opening the cracks. In fact, the McCauley brackets $\langle\cdot\rangle_+$ are defined as $\langle x\rangle_+ = \max\{0, x\}$. Therefore, this criterion is intended to be applicable for both tensile and compressive matrix failure.

2.2.2 Fibre kinking and splitting failure

The physics of axial compressive failure has been already discussed in different papers about LaRC criteria, such as the work by Davidson and Waas (2014). Kink-band formation is characterized by different stages: matrix splitting in between the fibers can be identified in and it is the result of the high shear stresses introduced by failure in the neighbouring plies. In general, the high localised shear stresses can also be introduced by manufacturing defects, such as fibre misalignments. The splitting promotes further bending of the fibres, which in turn results in more splitting. The bent fibres eventually break due to the combination of bending and compressive stresses, first at one end and then at the other, finally resulting in a kink band.

Experimental observations, suggest that kink bands are preceded by matrix failure and microbuckling is not necessarily the triggering factor for failure. Following the previous observations, fibre kinking is assumed to result from shear-dominated matrix failure in a misaligned frame, under significant longitudinal compression. However, if the longitudinal compression is not significant, the shear-dominated matrix failure on the misaligned frame results in fibre splitting but not necessarily in fibre kinking.

Experimental data provided in literature for combined longitudinal compression and in plane shear loadings suggest that fibre kinking only takes place for an absolute value of longitudinal compression greater than $X^C/2$. However, for longitudinal compression combined with transverse tension, experimental results indicate that no kink bands are formed if the magnitude of the longitudinal compression is lower than X^C .

The criteria proposed for fibre kinking (Pinho *et al.* 2012) and splitting use the same failure index equation written as:

$$FI_{KINK} = FI_{SPLIT} = \left(\frac{\tau_{23}^m}{S_T^{is} - \eta_T \sigma_2^m} \right)^2 + \left(\frac{\tau_{12}^m}{S_L^{is} - \eta_L \sigma_2^m} \right)^2 + \left(\frac{\langle\sigma_2^m\rangle_+}{Y_T^{is}} \right)^2 \quad (7)$$

where the stresses used are in a misalignment frame (superscript “m”). It is possible to see the rotated coordinate systems relevant for the description of a kink band in Fig. 1.

The analytical description is shown in Pinho *et al.* (2012).

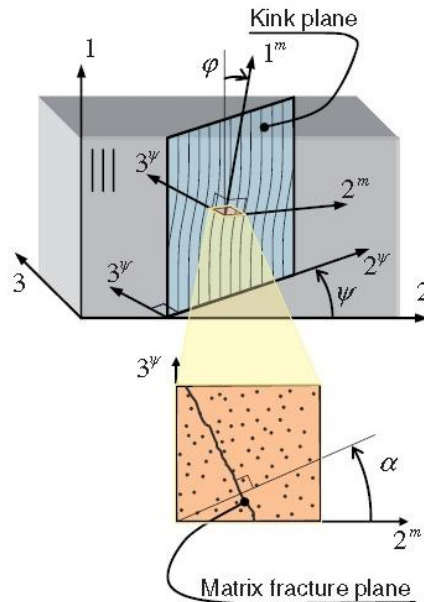


Fig. 1 Physical model for kink-band formation

3. Results

An API (Application Programming Interface) has been created between two software:

- Siemens Femap
- Visual Studio

With this, it is possible to evaluate failure index with different theories:

- Hoffman,
- LaRC05.

On the other hand, it allows one to calculate many margins of safety for sandwich panels:

- with composite skins (based on Hoffman's failure index),
- with metallic skins.

In both cases, the user can choose the source of stresses to be used. Indeed, they can be read directly from Femap output vector, that was read by Nastran output file, or they can be imported by an external file.

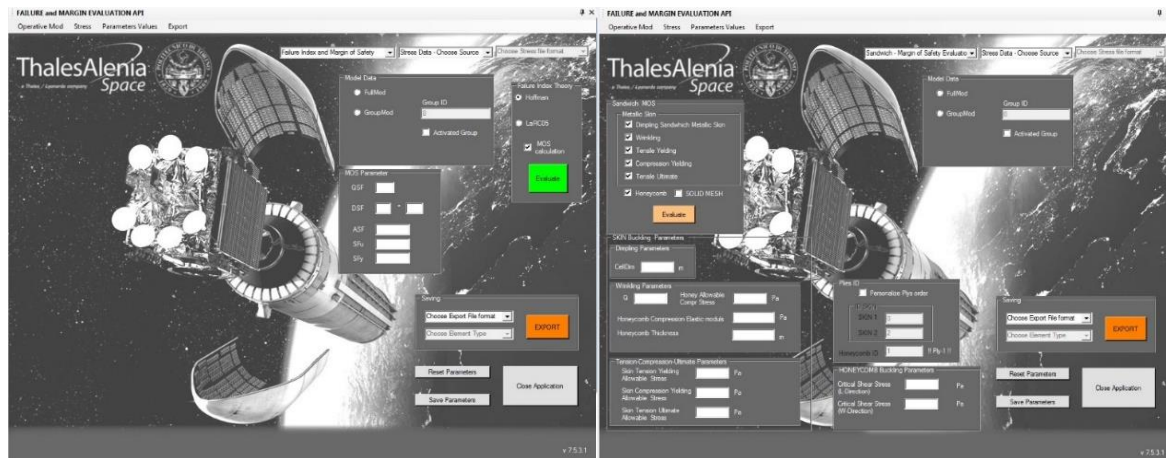
The strength of the API is a user friendly graphic interface, GUI (see Fig. 2), that allows to choose between two different activities:

- "Failure index operative mode" allows the users to evaluate failure index using different failure criteria.

In case of Hoffman's theory, the code is able to calculate the associated margin of safety. The API returns the contours for each single ply of the failure indexes for each element. Another plot is created with the maximum values of FI of the elements in all the plies.

- "Sandwich Panel – Margin of safety" operative mode allows to evaluate different margins of safety, MoS. It is divided in the calculation of MoS about skins, in particular metallic skin, and MoS of the honeycomb. For metallic skins, the user can select the different MoS below:

- Dimpling buckling



(a) Failure Index Operative Mode

(b) Sandwich Panel Operative Mode

Fig. 2 GUI

- Wrinkling buckling
- Tensile Yielding
- Compression Yielding
- Tensile Ultimate

While for the honeycomb, it is possible to evaluate MoS in the case it is meshed with a laminate element or solid elements.

Beyond the value of the margin of safety the application finds other useful information about the conditions of minimum MoS:

- Load case
- Element ID, basing on Femap model numeration
- Stress used in the calculation of the formula of margin of safety

The results given by the API have been validated by the comparison with results obtained by others tools. Hence, it was possible to verify that the implemented code worked correctly in all its functions.

To this aim, basic FEM models were created from time to time and analyzed using MSC Nastran. In particular, it was very important to check that the API was reading the correct properties of the model and the resulting stresses from analysis.

3.1 LaRC05 - validation

There were not commercial codes that evaluated LaRC05 failure index. So, it was necessary to use an alternative method to validate the written code. It has been created an Excel file (“FAILURE INDEX CALCULATION-LARC05.xlsx”), where failure indexes of each element for a ply was evaluated automatically. The file needs the data entry about material constants, the value of α_0 and the stress state of the model.

3.1.1 Model description

Now, to verify the algorithms in calculating FI the following example has been created: it is a 4-ply cantilever beam with a $[0^\circ/45^\circ/-45^\circ/0^\circ]$ ply lay-up clamped at one end and subjected to a

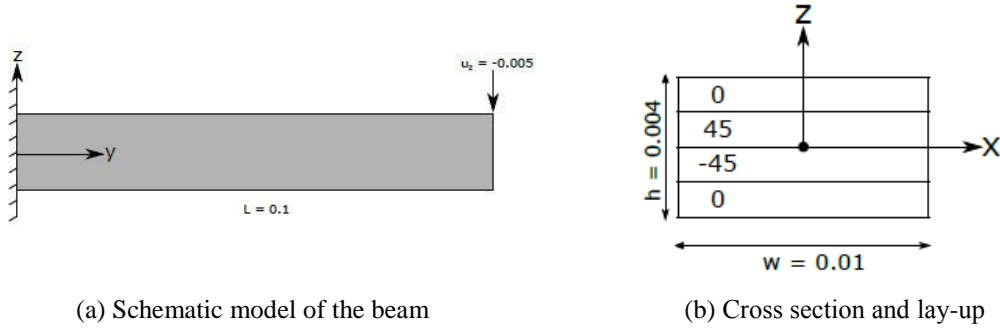


Fig. 3 Beam model

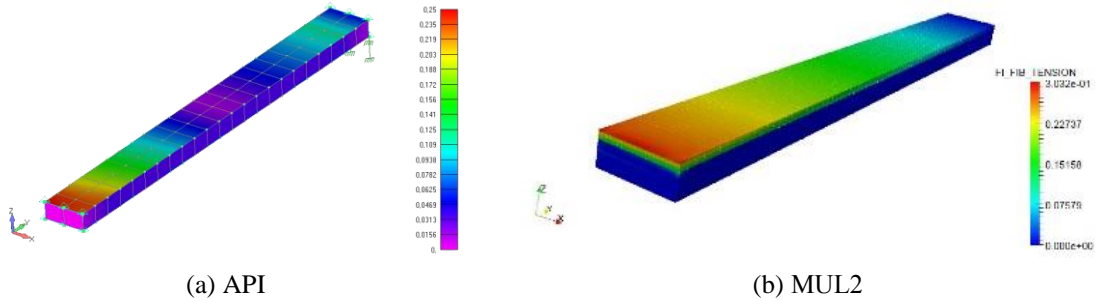


Fig. 4 Contour plot of the failure index for fibre failure under tension.

vertical deflection $U_z = 5$ mm at the free end. A schematic representation of the structure has been shown in Figs. 3(a)-(b) along with the geometric properties and applied boundary conditions.

The T300/PR319 material system has been considered for the current example, and its modelled material properties are listed below:

- $E_1 = 129.0$, $E_2 = 5.6$ GPa, $G_{12} = 1.3$ GPa, $\nu_{12} = 0.3$, $X_T = 1378.0$ MPa, $X_C = 950.0$ MPa, $Y_T = 40.0$ MPa, $Y_C = 125.0$ MPa, $S_L = 97.0$ MPa e $\alpha_0 = 53.0^\circ$;

In the following paragraph the results about ply 2 of the laminate has been reported.

3.1.2 Fiber tension

In this case, it was possible to compare API outputs with an additional source, in fact the model has been analyzed using the academic code MUL2. The failure index has been calculated in the middle plane of the beam. Both results have the same order of magnitude and they present a similar distribution along the longitudinal axis of the beam (See Fig. 4). The small difference in numerical values it would be caused by the different stress state evaluated by Nastran or MUL2 and the used mesh.

In Table 3 is presented the comparison between numerical values of failure index for some elements of the mesh. A perfect correlation has been reached.

The bolding value is the maximum failure index, as it was illustrated in Fig. 5. In this way it was controlled that the API was creating the correct contours from new output vectors.

Further, a last control has been realized comparing the distribution of stresses σ_x in Fig. 6 with the distribution of failure indexes. The reader can see that they are analogous, like it would be predictable on the basis of Eq. (5). In fact, where maximum stresses are reached, near the fixed ended, there are maximum failure indexes.

Table 3 Comparison of failure indexes for fibre failure under tension

| Element ID | API | Excel |
|------------|-----------------|-----------------|
| 143 | 0,214615 | 0.214615 |
| 145 | 0,224451 | 0.224451 |
| 148 | 0,16408 | 0.164080 |
| 250 | 0,148524 | 0.148524 |
| 253 | 0,198441 | 0.198441 |
| 254 | 0,187702 | 0.187702 |

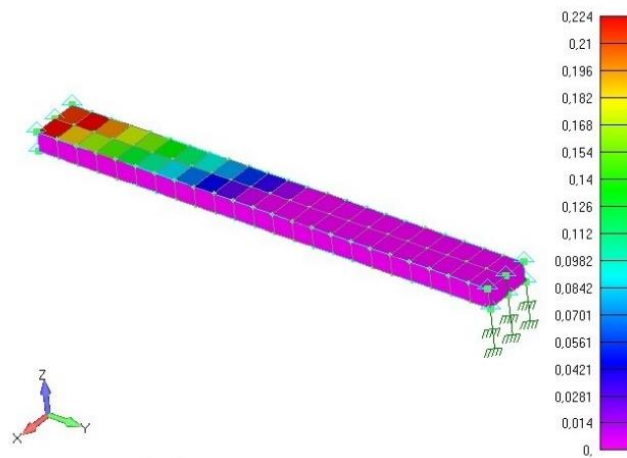


Fig. 5 Contour plot of the failure index for fibre failure under tension, created using API (not elements averaging)

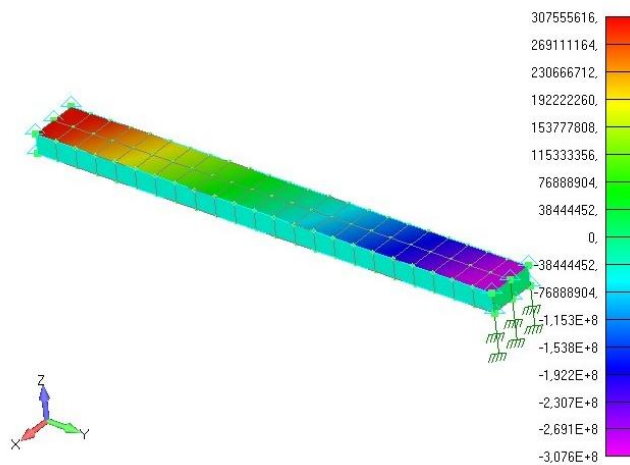


Fig. 6 Contour plot of the x normal stress, ply 2

Finally, it was verified the valuation of the overall maximum FI of each element. The following contour plot is obtained (See Fig. 7).

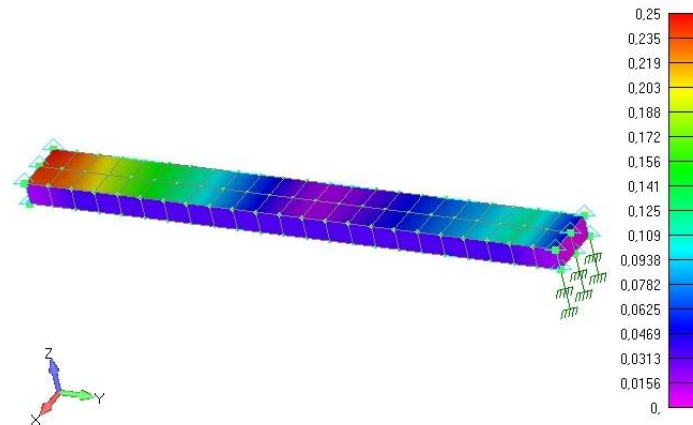


Fig. 7 Contour plot of the maximum failure index for fibre failure under tension for each element of the mesh

3.1.3 Matrix failure

The matrix failure of the laminate has been calculated for different angles α , to avoid useless repetitions of images. The case $\alpha=0^\circ$ is just reported in Fig. 8. However, all cases have been considered in numerical results presentation of Tables 4-5.

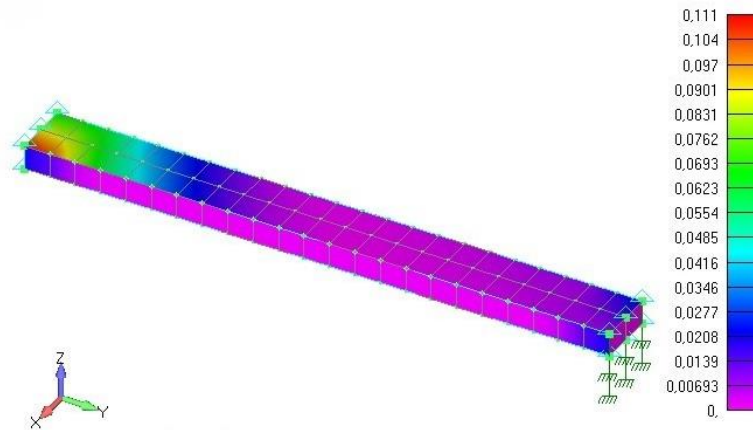


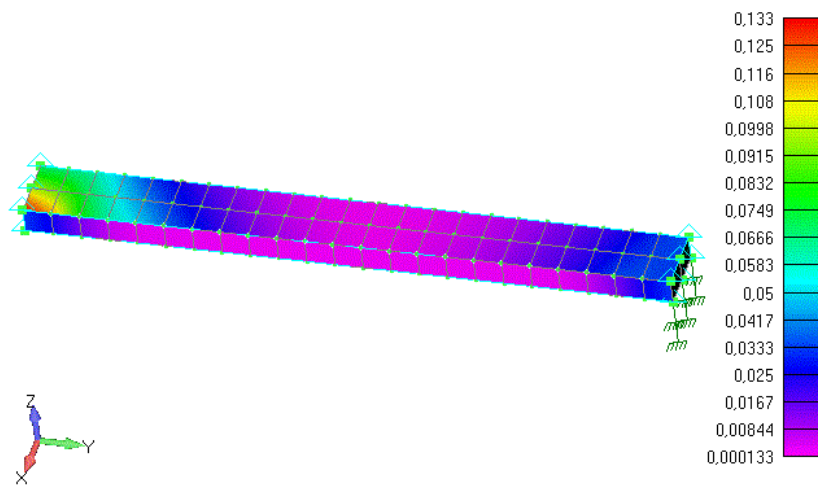
Fig. 8 Contour plot of the failure Index for matrix failure, $\alpha = 0^\circ$

Table 4 Comparison of Failure Indexes for matrix failure, API

| Element ID | 0° | 15° | 30° | 45° | 60° | 75° | 90° | 105° | 120° | 135° | 150° | 165° |
|------------|----------------|---------|---------|---------|---------|---------|---------|---------|---------|---------|---------|---------|
| 144 | 0.11084 | 0.07392 | 0.03924 | 0.01587 | 0.00164 | 0.00568 | 0.02402 | 0.05199 | 0.08966 | 0.12307 | 0.13995 | 0.13554 |
| 148 | 0.06642 | 0.05374 | 0.03547 | 0.01787 | 0.00571 | 0.00039 | 0.00202 | 0.01054 | 0.02580 | 0.04459 | 0.06092 | 0.06912 |
| 250 | 0.05603 | 0.06458 | 0.06282 | 0.05134 | 0.03421 | 0.01762 | 0.00642 | 0.00069 | 0.00205 | 0.00972 | 0.02290 | 0.04020 |
| 253 | 0.05676 | 0.04470 | 0.02860 | 0.01391 | 0.00431 | 0.00038 | 0.00265 | 0.01079 | 0.02465 | 0.04105 | 0.05458 | 0.06049 |
| 254 | 0.09739 | 0.10685 | 0.09962 | 0.07791 | 0.04901 | 0.02298 | 0.00673 | 0.00051 | 0.00563 | 0.02049 | 0.04521 | 0.07414 |

Table 5 Comparison of Failure Indexes for matrix failure, Excel

| Element ID | 0° | 15° | 30° | 45° | 60° | 75° | 90° | 105° | 120° | 135° | 150° | 165° |
|------------|----------------|---------|---------|---------|---------|---------|---------|---------|---------|---------|---------|---------|
| 144 | 0.11084 | 0.07392 | 0.03924 | 0.01587 | 0.00164 | 0.00568 | 0.02402 | 0.05199 | 0.08966 | 0.12307 | 0.13995 | 0.13554 |
| 148 | 0.06642 | 0.05374 | 0.03547 | 0.01787 | 0.00571 | 0.00039 | 0.00202 | 0.01054 | 0.02580 | 0.04459 | 0.06092 | 0.06912 |
| 250 | 0.05603 | 0.06458 | 0.06282 | 0.05134 | 0.03421 | 0.01762 | 0.00642 | 0.00069 | 0.00205 | 0.00972 | 0.02290 | 0.04020 |
| 253 | 0.05676 | 0.04470 | 0.02860 | 0.01391 | 0.00431 | 0.00038 | 0.00265 | 0.01079 | 0.02465 | 0.04105 | 0.05458 | 0.06049 |
| 254 | 0.09739 | 0.10685 | 0.09962 | 0.07791 | 0.04901 | 0.02298 | 0.00673 | 0.00051 | 0.00563 | 0.02049 | 0.04521 | 0.07414 |

Fig. 9 Contour plot of the failure index for kinking failure, $\alpha = 0^\circ$

In tables above it is possible observe that the results from the two methods have a good matching.

3.1.4 Kinking failure

Table 6 Comparison of Failure Indexes for kinking failure, API

| Element ID | API | Excel |
|------------|-----------------|-----------------|
| 143 | 0.067409 | 0.067409 |
| 144 | 0.132997 | 0.131957 |
| 145 | 0.063656 | 0.063615 |
| 146 | 0.098234 | 0.097921 |
| 147 | 0.055709 | 0.055742 |
| 148 | 0.063641 | 0.062987 |
| 250 | 0.0595642 | 0.0593553 |
| 251 | 0.0364779 | 0.0364761 |
| 252 | 0.0636411 | 0.0635637 |
| 253 | 0.0557091 | 0.0556161 |
| 254 | 0.0982335 | 0.0979206 |

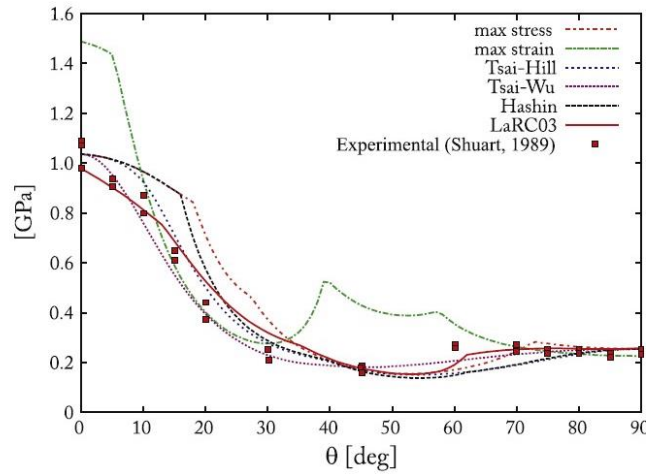


Fig. 10 Compressive strength as a function of ply orientation (LaRC03)

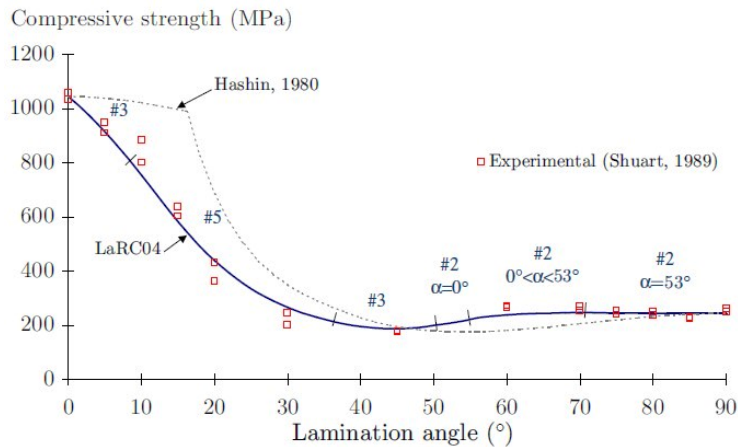


Fig. 11 Compressive strength as a function of ply orientation (LaRC04)

For the kinking failure of the structure, a good agreement of results between API and Excel has been obtained, as shown in Table 6. In fig. 9 the contour plot for $\alpha = 0^\circ$ is reported.

3.2 Common issues when using failure criteria and critical discussion

A detailed comparison between failure index obtained from classical criteria and previous version of LaRC criteria (LaRC03 and LaRC04) are reported by Nali and Carrera (2011), Dávila and Camanho (2003), Pinho *et al.* (2005) and Zhang *et al.* (2013). Now only some results obtained on cross-ply laminates (in AS4/3502) changing lamination angle are shown in Figs. 10-11.

A deeper attention was spent to show the difference between Hoffman criterion results and those calculated on the basis of LaRC05 theory. To do this, juxtaposition was used the API on models already analyzed for the validation. The current example in this paragraph is a sandwich panel with two composite multilayered plates as skins. This were made of two type of composite laminate named:

- Fabric,

Table 7 Lay-up

| Layup | | | |
|-------|-----------------|---------------|-------------|
| Ply | Material | Thickness (m) | Angle (deg) |
| 1 | Fabric | 0.000137 | 0 |
| 2 | M55J | 0.000127 | 0 |
| 3 | M55J | 0.000127 | -45 |
| 4 | M55J | 0.000127 | 90 |
| 5 | M55J | 0.000127 | 90 |
| 6 | M55J | 0.000127 | 45 |
| 7 | M55J | 0.000127 | 0 |
| 8 | M55J | 0.000127 | 0 |
| 9 | M55J | 0.000127 | 45 |
| 10 | M55J | 0.000127 | 90 |
| 11 | M55J | 0.000127 | 90 |
| 12 | M55J | 0.000127 | -45 |
| 13 | M55J | 0.000127 | 0 |
| 14 | Fabric | 0.000137 | 0 |
| 15 | 3/16-5056-0.001 | 0.0243 | 90 |
| 16 | Fabric | 0.000137 | 0 |
| 17 | M55J | 0.000127 | 0 |
| 18 | M55J | 0.000127 | -45 |
| 19 | M55J | 0.000127 | 90 |
| 20 | M55J | 0.000127 | 90 |
| 21 | M55J | 0.000127 | 45 |
| 22 | M55J | 0.000127 | 0 |
| 23 | M55J | 0.000127 | 0 |
| 24 | M55J | 0.000127 | 45 |
| 25 | M55J | 0.000127 | 90 |
| 26 | M55J | 0.000127 | 90 |
| 27 | M55J | 0.000127 | -45 |
| 28 | M55J | 0.000127 | 0 |
| 29 | Fabric | 0.000137 | 0 |

- M55J^a,

and the material 3/16-5056-0.001 was used as honeycomb.

The materials modeled in the examples have the following mechanical properties:

- Fabric - $E_1 = E_2 = 55$ GPa, $G_{12} = 5.5$ GPa, $\nu_{12} = 0.31$, $X_T = 690.0$ MPa, $X_C = 580.0$ MPa, $Y_T = 371.0$ MPa, $Y_C = 334.0$ MPa, $S_L = 107.0$ MPa e $\alpha_0 = 53.0^\circ$;

^a M55J is the name of carbon fiber; however, in this context, it is used to indicate the entire laminate plate made of it.

- M55J - $E_1 = 31.1$ GPa, $E_2 = 6.0$ GPa, $G_{12} = 4.0$ GPa, $\nu_{12} = 0.22$, $X_T = 1776.0$ MPa, $X_C = 29.9$ MPa, $Y_T = 714.0$ MPa, $Y_C = 125.0$ MPa, $S_L = 56.0$ MPa e $\alpha_0 = 53.0^\circ$;
 - 3/16-5056-0.001 - $E_1 = E_2 = 1000.0$ GPa, $G_{12} = 0.001$ GPa, $\nu_{12} = 0.001$, $X_T = X_C = Y_T = Y_C = S_L = 1E+15$ MPa e $\alpha_0 = 53.0^\circ$;
- The complete lay-up has been shown in Table 7:

A graphical comparison will be done using failure index of each element of the mesh contours.

Figs.12-13 show results for ply 13. It is possible to observe that the trends of failure index obtained with Hoffman and LaRC05 criteria are similar, but there is a great difference in the numerical values. This difference is generated by the fact that LaRC05 criteria describes more accurately the physics of failure phenomena in composites and it is based on a 3D description of the stress state in the structure; therefore, it is less conservative than Hoffman criteria.

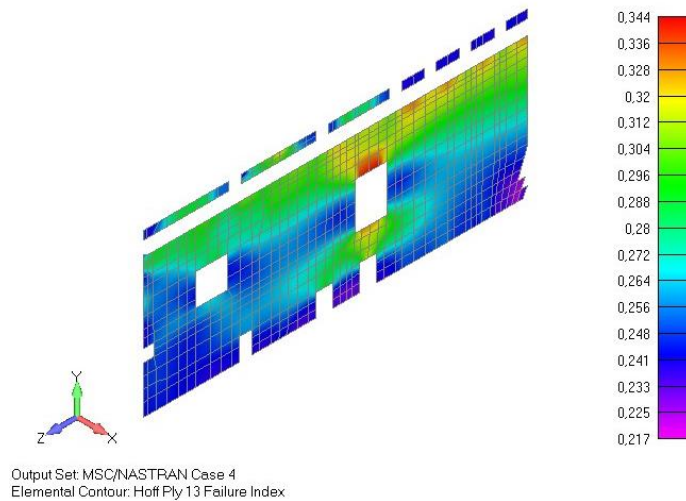


Fig. 12 Contour of Hoffman's failure indexes, Ply 13

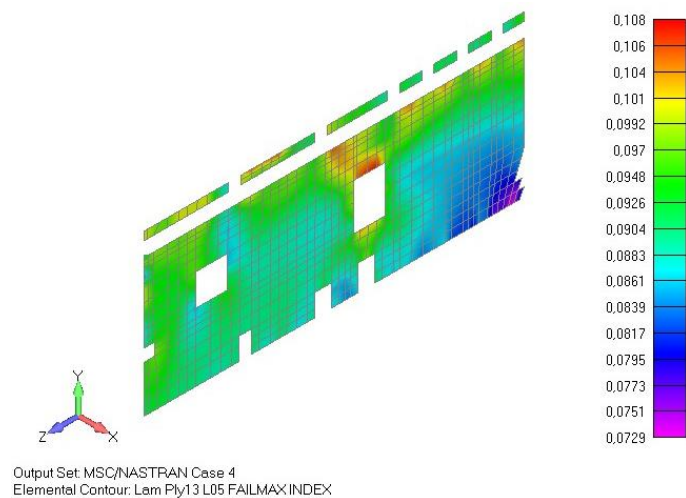


Fig. 13 Contour of LaRC05's failure indexes, Ply 13

The committed discrepancy between the two criteria, Δ , is equal to:

$$\Delta = \frac{|FI_{max_{LaRC05}} - FI_{max_{Hoff}}|}{|FI_{max_{Hoff}}|} * 100 = \frac{|-0.236|}{|0.344|} * 100 = 68.60\% \quad (8)$$

4. Concluding remarks

The progress in the use of composites materials is greatly influenced by the capability of expecting and understanding their failure mode. Many different theories have been thought and developed for this purpose. However, some of these are not enough accurate since they are based on assumptions valid for metallic structures or on a reduced knowledge of failure phenomena.

At the current state of the art, the NASA Langley Research Center worked out a series of criteria, which obtained a significant correlation with real example. These were known as LaRC criteria, and the last criterion developed is the LaRC05.

However, these new criteria are not embedded in most commercial software used in industry. In this context, the API AMOSC (Automatic Margin Of Safety Calculation) was implemented using Visual Basic language and embedded into Femap Siemens SW.

It allows to evaluate failure index according to LaRC05 criterion, starting from the stress field calculated by a finite element code. However, the user can employ it to calculate also failure index by referring to the classical Hoffman criterion and considering different margin of safety for sandwich panels.

This tool is largely validated using different simply study cases, some of them based on pre-existing real structure.

After the implementation, it was possible to compare and discuss results produced by passing from Hoffman to LaRC05 on the same structure considered for validation.

Finally, the capability to use more accurate stress fields, obtained by higher-order kinematic theories, in the calculation of failure index was implemented (in a beginning form) in the API. The refinement of this function can be a future development and improvement of the work presented in this paper.

Acknowledgments

The research described in this paper was supported by Thales Alenia Space.

References

- Davidson, P. and Waas, A.M. (2014), "Mechanics of kinking in fiber-reinforced composites under compressive loading", *J. Compos. Mater.*, **21**(6), 667-684.
- Dávila, C.G. and Camanho, P.P. (2003), "Failure criteria for FRP laminates in plane stress"; L-19012, NASA Langley Research Center, U.S.A.
- Deuschle, H.M. and Puck, A. (2013), "Application of the Puck failure theory for fibre-reinforced composites under three-dimensional stress: Comparison with experimental results", *J. Compos. Mater.*, **47**(6-7), 827-846.

- Grasso, A. (2018), "Implementation of classical and advanced failure criteria for composite layered structures in FEMAP and assessment of results", M.Sc. Dissertation, Politecnico di Torino, Torino.
- Hoffman, O. (1967), "The brittle strength of orthotropic materials", *J. Compos. Mater.*, **1**(2), 200-206.
- Kaddour, A.S. and Hinton, M.J. (2012), "Benchmarking of triaxial failure criteria for composite laminates: Comparison between models of 'Part (A)' of 'WWFE-II'", *J. Compos. Mater.*, **46**(19-20), 2595-2634.
- Kaddour, A.S. and Hinton, M.J. (2013), "Maturity of 3D failure criteria for fibre-reinforced composites: Comparison between theories and experiments: Part B of WWFE-II", *J. Compos. Mater.*, **47**(6-7), 925-966.
- Kaddour, A.S., Hinton, M.J., Smith, P.A. and Li, S. (2013), "The background to the third world-wide failure exercise", *J. Compos. Mater.*, **47**(20-21), 2417-2426.
- Nali, P. and Carrera, E. (2011), "A numerical assessment on two-dimensional failure criteria for composite layered structures", *Compos. Part B Eng.*, **43**(2), 280-289.
- Pinho, S.T., Darvizeh, R., Robinson, P., Schuecker, C. and Camanho, P.P. (2012), "Material and structural response of polymer-matrix fibre-reinforced composites", *J. Compos. Mater.*, **46**(19-20), 2313-2341.
- Pinho, T., Dávila, C.G., Camanho, P.P., Iannucci, L. and Robinson, P. (2005), "Failure models and criteria for FRP under in-plane or three-dimensional stress states including shear non-linearity"; L-19089, NASA Langley Research Center, U.S.A.
- Raghava, R., Caddell, R.M. and Yeh, G.S.Y. (1973), "The macroscopic yield behavior of polymers", *J. Mater. Sci.*, **8**(2), 225-232.
- Zhang, D., Xu, L. and Ye, J. (2013), "Prediction of failure envelopes and stress-strain curves of fiber composite laminates under triaxial loads: Comparison with experimental results", *J. Compos. Mater.*, **47**(6-7), 763-776.